

Isocost lines describe the cellular economy of genetic circuits

Andras Gyorgy¹, José I. Jiménez^{2,3}, John Yazbek^{4,5}, Hsin-Ho Huang³, Hattie Chung⁶,
Ron Weiss^{4,5}, Domitilla Del Vecchio^{3,5,*}

1. Department of Electrical Engineering and Computer Science, Massachusetts Institute of Technology, Cambridge, MA, USA.
2. Faculty of Health of Medical Sciences, University of Surrey, Guildford, UK.
3. Department of Mechanical Engineering, Massachusetts Institute of Technology, Cambridge, MA, USA.
4. Department of Biological Engineering, Massachusetts Institute of Technology, Cambridge, MA, USA
5. Synthetic Biology Center, Massachusetts Institute of Technology, Cambridge, MA, USA
6. Harvard Medical School, Boston, MA, USA.

Abstract

Genetic circuits in living cells share transcriptional and translational resources that are available in limited amounts. This leads to unexpected couplings among seemingly unconnected modules, which result in poorly predictable circuit behavior. Here we determine these interdependencies between products of different genes by characterizing the economy of how transcriptional and translational resources are allocated to the production of proteins in genetic circuits. We discover that, when expressed from the same plasmid, the combinations of attainable protein concentrations are constrained by a linear relationship, which can be interpreted as an isocost line, a concept used in microeconomics. We created a library of circuits with two reporter genes, one constitutive and the other inducible in the same plasmid, without a regulatory path between them. In agreement with the model predictions, experiments reveal that the isocost line rotates when changing the RBS strength of the inducible gene and shifts when modifying the plasmid copy number. These results demonstrate that isocost lines can be employed to predict how genetic circuits become coupled when sharing resources and provide design guidelines for minimizing the effects of such couplings.

Received for publication: Final form date:

* Corresponding Author: Domitilla Del Vecchio, ddv@mit.edu

Introduction

The ability to predict the behavior of a system from that of the composing modules is a core problem in systems and synthetic biology (1, 2). However, prediction accuracy is still limited as modules display context-dependent behavior, wherein the function of circuits is affected by direct or indirect interactions with surrounding cellular components and resources (3). One cause of context-dependence is the fact that different circuits share common cellular resources that are available in limited amounts. When new genes are introduced into a cell, resources involved in their expression have to be redirected. In the model organism *Escherichia coli*, the additional demand for resources, such as nucleotides, tRNAs, ribosomes, and RNA polymerase, may lower cell fitness by, for instance, affecting the growth rate of the cell (4–9). Furthermore, over-expressing one gene reduces the availability of resources and, as a consequence, decreases expression of other genes (10). This couples the expression of genes that do not have a direct regulatory link between them. These studies suggest that the cellular economy of gene expression, understood as the distribution of limited cellular resources to different genes, plays an important role in the behavior of genetic circuits.

Among the cellular resources required for gene expression, RNAP and ribosomes are determining factors. Accordingly, studies have focused on determining how RNAP and ribosomes are distributed depending on the growth rate, used as a general

descriptor of the status of the cell (6, 8). Experiments performed by changing DNA concentration demonstrated that transcription is limited by the available amount of RNAP (11). Similarly, it has been shown that the availability of ribosomes is the major limiting factor in the translation process and one of the reasons why mRNA levels often do not correlate with the concentration of proteins produced in the cell (10). These findings indicate that RNAP and ribosomes are key transcriptional and translational resources that determine the cellular economy of gene expression. Therefore, characterizing how the products of different genes become coupled due to sharing limited amounts of ribosomes and RNAP is essential both for understanding the behavior of natural circuits and for engineering new ones.

In this paper, we assembled a system with two fluorescent reporter proteins, one inducible (RFP) and one constitutive (GFP) without a regulatory path between them on the same plasmid, for several combinations of plasmid copy number and RBS strength for the inducible gene (Fig 1A). Combining experiments on synthetic constructs with a mechanistic model, we discover that the coupling between two gene products located on the same plasmid but without a regulatory link between them is captured by a linear relationship. This relationship can be interpreted as an isocost line, already employed in microeconomics to describe how two products can be purchased with a limited budget (12). This isocost line explicitly indicates how the extent of coupling depends on relevant parameters, such as RBS strength and plasmid copy number, and provides a simple tool to optimize circuits such that the extent of coupling is minimized.

Materials and methods

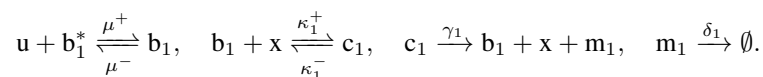
Bacterial strains, cell culturing and fluorescence determination

Standard molecular biology techniques were used to prepare the different constructions in *E. coli* DH5 α (see SI Sections A1 and A2 for details). All experiments were performed using the DIAL strains harboring the cassette JTK160 in *E. coli* MC1061 (13). Growth conditions were selected to maximize the antagonistic effect of the inducible reporter into the constitutive. Pre-starting cultures coming from isolated colonies in LB plates were grown in 24-well plates using 1 ml of M9 minimal medium supplemented with 0.4% glucose, 0.2% casamino acids, 1 mM thiamine, ampicillin (100 μ g/ml) and kanamycin (50 μ g/ml). Cells were incubated for 8-10 h at 30 °C and 100 rpm in an orbital shaker. When they reached the mid-log phase, they were diluted (1/200) into 1 ml of the same M9 fresh media and incubated under the same conditions. Four hours after dilution, during exponential growth, the cultures were induced with AHL (Cayman Chemical, Ann Arbor, MI) at a final concentration of 1, 2, 4, 10 and 1000 nM, and cells were grown for 8 additional hours until they reached the steady state of protein production, still in the exponential phase of growth. Unless explicitly stated (see Fig. S6-S8), the cultures were not induced with aTc.

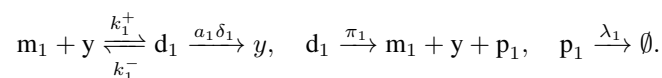
For single-cell analysis, 5-10 μ l aliquots were taken from each well every 1 h. The volume of the culture was kept constant replenishing with the same volume of fresh medium. Right after removal, the aliquots were diluted in 100 μ l of water and analyzed in a BD Accuri C6 flow cytometer (BD Biosciences, San Jose, CA). The instrument is equipped with blue (488 nm) and yellow-green lasers (552 nm) for GFP and RFP, respectively. Emission was detected using a 525/50 filter for GFP and a 610/20 for RFP. Flow rates were always kept below 1000 events/sec and 30,000 to 100,000 events were analyzed in each read. Daily calibrations of the flow cytometer were performed using Spherotech 6 peak validation beads (BD Biosciences, San Jose, CA). To track the behavior of the whole population present in each well, the same plate was monitored every 20 minutes for absorbance (600 nm) in a Synergy MX (Biotek, Winooski, VT) plate reader.

Mathematical model

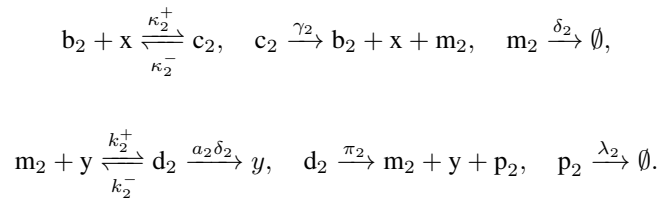
Module 1 in Fig 1A consists of a single gene expressing protein p_1 (RFP) upon induction by the active transcription factor u (LuxR-AHL complex). In particular, promoter complex b_1 is formed by u binding to the empty promoter b_1^* of the gene encoding p_1 , so that the binding of RNAP x can form the transcriptionally active promoter complex c_1 , resulting in the production of mRNA m_1 encoding p_1 at rate γ_1 (encompassing the elongation reactions), which further decays at rate δ_1 :



Translation of p_1 is initialized by the ribosome y binding to the RBS of the mRNA m_1 , forming the translationally active complex d_1 . Protein p_1 is degraded at rate λ_1 , whereas elongation and production are lumped together in one step with effective production rate π_1 :



Module 2 in Fig 1A consists of a single gene expressing protein p_2 constitutively, that is, the production of p_2 can be described with the reactions



Since the total concentration of DNA is constant (14), we further have the conservation laws $n = b_1^* + b_1 + c_1 = b_2 + c_2$, where n is the plasmid copy number.

The experimental data presented in Fig 1B demonstrates that while the expression of a gene (gapA) affects that of another gene on the same plasmid (RFP), it has no effect on the steady state expression of a third gene located on the chromosome (GFP), for details see Figs S2-S8. This indicates a separation between the resources available to the genes on the plasmid and those available to the chromosomal genes. To appropriately capture this by the model, we let X and Y represent the concentration of RNAP and ribosomes, respectively, available to the genes on the plasmid. We then write the conservation laws $X = x + c_1 + c_2$ and $Y = y + d_1 + d_2$, where x and y denote the free concentrations of RNAP and ribosomes, respectively, whereas c_i and d_i represent the concentration of RNAP and ribosome bound in module i ($i = 1, 2$). The separation of resources is not required for the existence of the isocost line and it only affects the extent of coupling between the expression levels of the two genes. The SI Part B contains the details on the model and on the mathematical derivations leading to the isocost line, together with the simulation results.

Results

Rationale of the circuit

We created a set of circuits that encode the expression of fluorescent reporters GFP and RFP to study how expression of one gene (RFP) affects that of the other (GFP) in *E. coli* cells (MBP-1.0; Fig 1A). GFP is produced constitutively whereas RFP is expressed only in response to AHL input, which binds the transcriptional activator LuxR. Each gene is encoded as an independent transcriptional module isolated from the others with double terminators. The plasmid also contains a ColE2-type origin of replication regulated by the RepA protein encoded in the bacterial chromosome. This enables us to dynamically control the plasmid copy number using the DIAL system of hosts (13). For a detailed description of the circuit and its components, see Fig S1.

In a typical time course experiment we track, using flow cytometry, the expression of both reporters in cells growing in glucose 0.4% as the sole carbon source. Cells are kept in the exponential phase for the complete duration of the experiment from AHL induction and until the steady-state of protein production is reached (see Materials and methods). By monitoring the population at the single cell level we confirmed the absence of subpopulations of mutants not expressing the fluorescent genes that could interfere with our observations. Under these conditions, the circuit initially expresses GFP and LuxR. Induction with AHL results in an increase in the concentration of RFP while the concentration of GFP should in principle remain constant. However, we observe experimentally that as the concentration of RFP increases, the concentration of GFP decreases (Fig 1A).

Experiments with both genes on the same plasmid allow us to rule out competition for factors involved in DNA replication, which may affect the relative abundance of reporters placed in separate replicons. We considered several alternative reasons beyond competition for cellular resources that could explain our observation, but all of them were discarded by control experiments as explained in what follows.

First, we focused on the two reporter genes used in this study, GFP and RFP. We checked possible effects on GFP fluorescence emission that could be affected by RFP excitation. We compared the fluorescence emission spectrum for the GFP channel of control cells containing or lacking RFP and the results are identical (Fig S9). Furthermore, we swapped the two reporter genes (Fig S10) and observed the same phenomenon as in Fig 1A (for details see Figs S11-S14), leading to the conclusion that the results are not due to the fluorophore choice.

Second, we constructed MBP-chrom depicted in Fig 1B by modifying MBP-1.0 (Fig 1A) such that it contains genes encoding RFP and glyceraldehyde 3-phosphate dehydrogenase (*gapA*; accession no. NC_000913.2) in place of GFP and RFP, respectively. GapA is one of the most abundant endogenous proteins in the cytoplasm of *E. coli* growing on glucose (15) since it catalyzes one of the key steps of glycolysis, the conversion of glyceraldehyde 3-phosphate into 1,3-biphosphoglycerate (16). Furthermore, we inserted the Ptet-GFP cassette of MBP-1.0 (Fig 1A) into the chromosome. While the expression of GapA

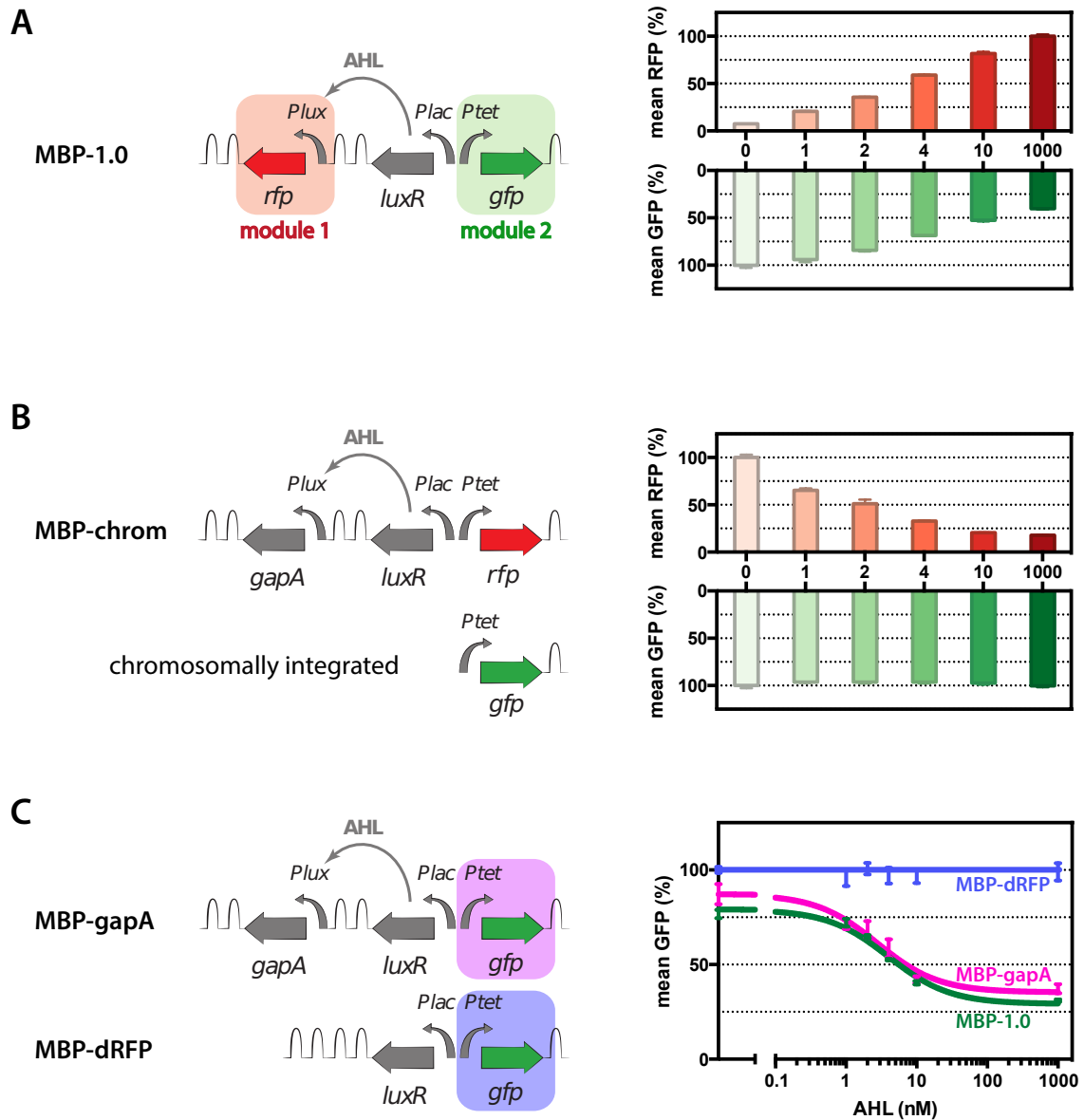


Figure 1: Rationale of the circuit. (A) On the left, schematic representation of the construct used to study the cellular economy of genetic circuits. GFP is constitutively expressed and RFP is under the control of activator LuxR and input AHL. Curved arrows and hairpins represent promoters and terminators, respectively (for details see Fig S1). On the right, the mean fluorescence levels at the steady state are presented for the indicated concentrations of AHL (nM), normalized to the values with no AHL (for details see Fig S15). (B) On the left, schematic representation of the construct used to study the separation of the pool of resources used by the plasmid and by the chromosomal genes. On the right, the mean fluorescence levels at the steady state are presented for the indicated concentrations of AHL (nM), normalized to the values with no AHL (for details see Fig S2-S5). We also constructed MBP-tetR with the chromosomally integrated GFP together with constitutively expressed TetR on a plasmid (for details see SI Section A2) to demonstrate that possible reductions to the chromosomal GFP expression are detectable (for details see Figs S6-S8). (C) In the control circuit MBP-gapA, the RFP gene of MBP-1.0 has been replaced by the glyceraldehyde dehydrogenase encoding gene (*gapA*) from *E. coli*. MBP-dRFP does not contain RFP. On the right, GFP dose response plots for the circuit MBP-1.0 and the controls MBP-gapA and MBP-dRFP (for details see Fig S15). All data plots represent mean values and standard deviations of populations in the steady state analyzed by flow cytometry in three independent experiments.

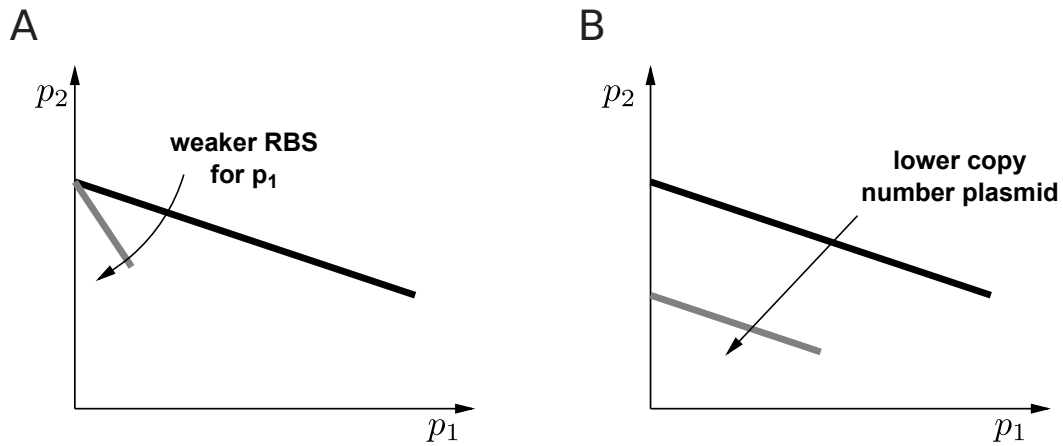


Figure 2: Isocost lines predicted by the model. (A) Decreasing the RBS strength of RFP (p_1), that is, increasing the dissociation constant k_1 , rotates the isocost line clockwise. (B) Decreasing the plasmid copy number n shifts the isocost line down.

decreases that of RFP expressed from the same plasmid, it does not affect the expression of GFP integrated into the chromosome (Fig 1B). This indicates that the pools of RNAP and ribosomes available to the genes on the plasmid are essentially separated from those available to the chromosomal genes.

Finally, we built two control circuits, MBP-gapA and MBP-dRFP (Fig 1C) by modifying MBP-1.0 (Fig 1A): MBP-gapA contains a gene encoding GapA in place of RFP, whereas MBP-dRFP lacks the RFP gene. We examined the production of GFP and RFP for circuits MBP-1.0, MBP-gapA and MBP-dRFP in assays using different concentrations of inducer AHL. Induction of GapA with AHL has the same effect on GFP as inducing RFP, decreasing GFP production by up to 60% (Fig 1C). This indicates that the GFP decrease is not due to the product RFP itself but rather to the process that produces RFP. Synthesis of GFP is not affected in the MBP-dRFP control, where RFP is not produced, indicating that it is not the transcriptionally active complex AHL-LuxR that has direct effect on GFP but it is the gene expression process induced by this complex that affects GFP (for details see Figs S15-S17). Taken together, the above results indicate that the decrease in GFP production upon RFP induction in MBP-1.0 (Fig 1A) is due to the competition for RNAP and ribosomes caused by the production of RFP and not by the product RFP itself.

Isocost lines describe the allocation of limited cellular resources

We considered a mechanistic model of the synthetic circuit of Fig 1A to understand how limited amounts of RNAP and ribosomes yield the experimental results in Fig 1A (for details, see Materials and methods and SI Part B). Using this model, we characterize the effect that module 1 producing p_1 (RFP) has on p_2 (GFP) in module 2. Specifically, we determine how this effect depends on the dissociation constant k_i of the RBS of p_i and on the plasmid copy number n . The concentration of available RNAP and ribosomes is denoted by X and Y , respectively.

By analyzing this model, we obtain that the attainable output (p_1, p_2) of the synthetic circuit in Fig 1A satisfies the formula:

$$\alpha p_1 + \beta p_2 = Y, \quad (1)$$

where α and β are lumped constants incorporating the system parameters (for details, see SI Section B3). The linear constraint in (1) can be interpreted as follows. With the available budget Y of ribosomes, the cell can produce p_1 units of p_1 at price α and p_2 units of p_2 at price β . When p_1 is uninduced, the pair (p_1, p_2) lies on the p_2 -axis ($p_1 = 0$), and as we increase the level of induction of p_1 , we move along a line from left to right (dark line in Fig 2), increasing p_1 and simultaneously, decreasing p_2 , according to (1). Using the conceptual analogy with microeconomics (12), we can interpret (1) as an isocost line.

The prices α and β of p_1 and p_2 increase with the dissociation constants k_1 and k_2 , respectively (see SI Section B3), where k_i is the dissociation constant of the ribosome binding to the RBS of the p_i . That is, the price of p_i decreases by increasing the strength of the corresponding RBS. Therefore, the isocost line rotates clockwise by decreasing the RBS strength of p_1 (Fig 2A). Hence, producing an extra molecule of p_1 leads to a larger effect on the concentration of p_2 . This seemingly counter-intuitive fact can be explained as follows. To attain the same protein concentration p_1 with a weaker RBS for p_1 (greater k_1)

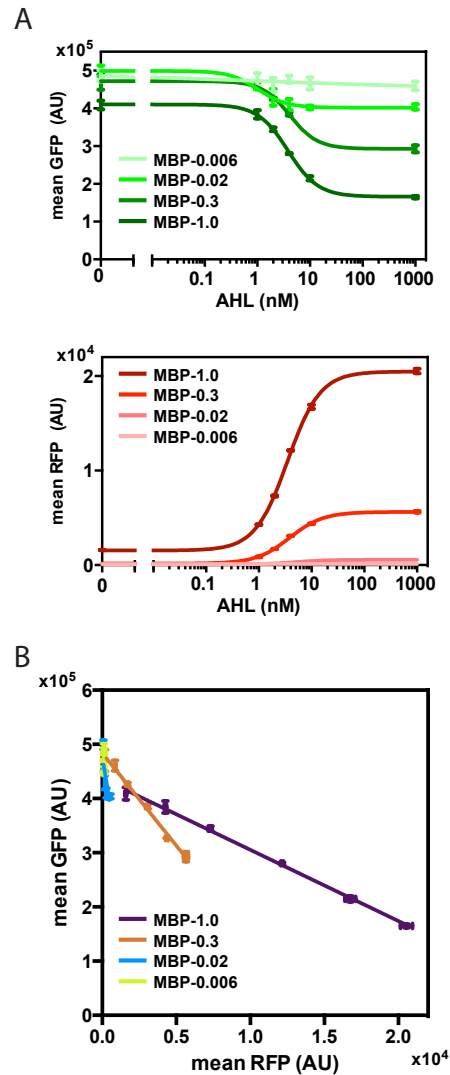


Figure 3: Influence of the RBS strength of RFP on the isocost line. (A) AHL dose response plots of GFP (upper) and RFP (lower) when RFP RBS strength is changed. The numbers indicate the relative strength of the RBS for RFP compared to MBP-1.0. (B) Linear relationships between GFP and RFP production. The steady state values of GFP are represented as a function of the values of RFP in the same experiment. For numerical simulation results, see Section B4 in SI Part B. All plots represent mean values and standard deviations of populations in the steady state analyzed by flow cytometry in three independent experiments (for details see Fig S18).

requires more mRNA, thus an increased usage of RNAP, and the same usage of ribosomes (see SI Section B3). Consequently, less RNAP is available for the production of p_2 , which, with the same amount of available ribosomes, leads to a smaller value of p_2 . This, in turn, implies a steeper isocost line.

The plasmid copy number n enters (1) via β as it decreases with n (see SI Section B3). Hence, the price β of p_2 increases as the plasmid copy number n decreases, since more ribosomes are required to produce the same amount of p_2 (due to decreased mRNA concentration). By contrast, the price α of p_1 does not depend on the plasmid copy number n , because p_1 is inducible. In fact, the demand of p_1 for RNAP and ribosomes is determined by the concentration of induced p_1 promoter, which depends on two factors: the plasmid copy number n and the concentration of the inducer of p_1 . Low copy number and high induction results in the same demand for RNAP and ribosomes as high copy number and low induction (so that the concentration of induced promoters are equal). Production of an extra molecule of p_1 thus requires the reallocation of the same amount of resources, so that the price of p_1 is independent of n . Referring to (1), since β decreases with n and α is independent of n , a

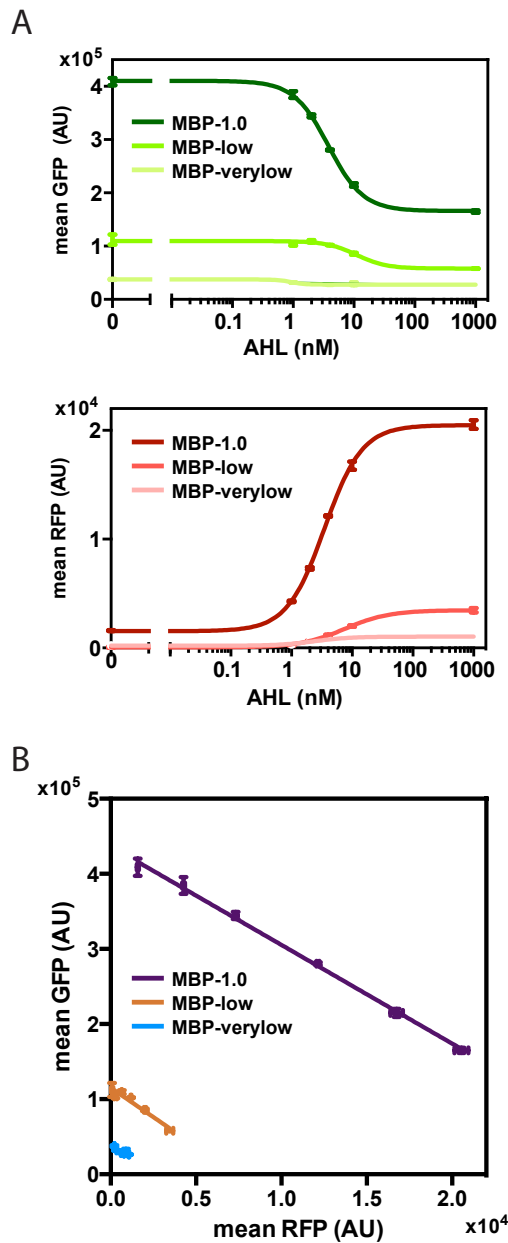


Figure 4: Influence of the plasmid copy number on the isocost line. (A) AHL dose response plots of GFP (upper) and RFP (lower) when plasmid copy number is changed. The plasmid MBP-1.0 was tested in the DIAL hosts JTK60 J (64 ± 2 copies), H (18 ± 4 copies) and E (4 ± 1 copies). These copy numbers lead to 60%, 48%, and 29% change in GFP, respectively. (B) Linear relationships between GFP and RFP production. The steady state values of GFP are represented as a function of the values of RFP in the same experiment. For numerical simulation results, see Section B4 in SI Part B. All plots represent mean values and standard deviations of populations in the steady state analyzed by flow cytometry in three independent experiments (for details see Fig S23).

fixed p_1 allows more p_2 for a greater n . As a result, the isocost line shifts downward by decreasing the plasmid copy number n (Fig 2B).

The prices α and β of p_1 and p_2 , respectively, decrease as the total concentration X of RNAP increases, so that the same budget Y allows the production of more p_1 and p_2 (as a result of increased mRNA concentration). Similarly, keeping the prices α and β fixed and increasing the budget Y yields more p_1 and p_2 (as a result of increased ribosome concentration).

Experimental validation of isocost lines

We validated the theoretical predictions in experiments where either the RBS of RFP (Fig 3) or the copy number of the circuit were modified (Fig 4). We therefore created a set of circuits with progressively weaker RBS strength for the RFP gene using a set of RBS sequences that range from very strong (MBP-1.0) to very weak undetectable translation of RFP (MBP-0.006) (See Tab S3 for sequences, nominal, predicted and observed strength values of the RBSs tested). The dose response curves show that weaker RBS strengths have reduced effects on GFP, with no appreciable effect in the case of MBP-0.006 (Fig 3A, for details see Fig S18). This experimental observation correlates well with numerical simulations of the model, which accounts for the conservation of ribosomes and RNAP along with the usual production and degradation of mRNAs and proteins (Fig 3 and Fig S28). The parameters used in the model were obtained from the literature (see Tabs S4–S5 for details). When plotting GFP over RFP we observe, as predicted by the isocost line (1), a linear relationship between RFP and GFP productions (Fig 3B). Further, when the RBS of RFP becomes weaker, we observe that the slope becomes steeper (Fig 3B). This is in agreement with the prediction based on the isocost line (1). In the experimental isocost lines, the intercept is higher for weaker RBSs of RFP. Further inspection revealed that there is production of RFP in the absence of AHL (Fig S21) due to a basal level of transcription from *Plux*. Because of the coupling, circuits with stronger RBSs for RFP have lower initial values for GFP in the absence of AHL.

In addition to the original copy number of the plasmid MBP-1.0, we analyzed two lower plasmid copy numbers. Instead of replacing the origin of replication, which may in turn generate artifacts due to the involvement of different replication machinery for each of the origins, we used the DIAL strains (13). For these experiments we always used the original MBP-1.0 construct but changed the DIAL host, to tune the number of copies of the circuit. The nominal exponential phase plasmid copy numbers were 64 ± 2 (J, medium), 18 ± 4 (I, low) and 4 ± 1 (E, very low) according to (13). The results in Fig 4A show that the decrease in GFP production depends on the number of copies of the plasmid and the corresponding percentage change is 48% and 29% for low and very low copy numbers, respectively (for details see Fig S23). Numerical simulations are consistent with the experimental data (Fig 4 and Fig S29). The parameters used in the model were obtained from the literature (see Tabs S4–S5 for details). When plotting the production of GFP as a function of RFP, we observe that the isocost lines shift down as the copy number decreases in agreement with the theoretical predictions (Fig 4B).

Realizable region and minimizing circuit coupling

Using the isocost lines, we next investigate how to design module 1 in Fig 1A so that when induced, its effects on module 2 are minimized. Specifically: How to choose the plasmid copy number n and the dissociation constant k_1 of the RBS of p_1 so that we minimize the sensitivity of p_2 to p_1 , such that (p_1, p_2) is fixed?

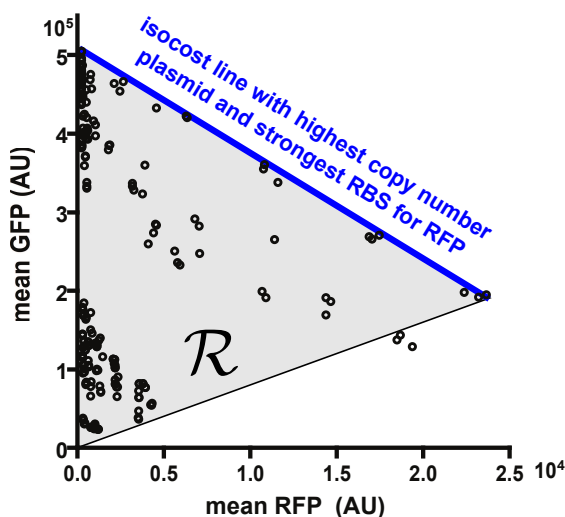


Figure 5: Realizable region of protein concentration. The theoretically predicted realizable region \mathcal{R} is denoted by the grey triangle, which is defined by the origin and the isocost line corresponding to (N, K) , depicted in blue. Experimental datapoints are also shown in the figure. The isocost line starts on the p_2 -axis but never reaches the p_1 -axis, since some small amount of RNAP and thus ribosomes will still be allocated for p_2 .

The design constraints are as follows. The plasmid copy number can vary between zero and its maximal value N . Similarly, the RBS strength of p_1 varies between zero and its maximal value, so that the corresponding dissociation constant is between a minimal value denoted by K and infinity. Consequently, we call $\mathcal{D} = [0, N] \times [K, \infty)$ the design space. With this, it can be shown that the pairs (p_1, p_2) that are realizable belong to the triangle \mathcal{R} defined by the origin and by the isocost line corresponding to (N, K) , depicted in Fig 5, matching the experimental data. For details, see SI Section B5.

The sensitivity of p_2 to p_1 is given by $\Delta p_2 / \Delta p_1 = \alpha / \beta$. This can be minimized by decreasing α and/or increasing β . The price α of p_1 can be minimized by picking $k_1 = K$, corresponding to the strongest RBS for p_1 . The value of β can be increased by decreasing the plasmid copy number n . Since smaller k_1 requires smaller n to attain the same (p_1, p_2) (see SI Section B5.2), the sensitivity is minimized for the strongest RBS for p_1 and the corresponding plasmid copy number that attains the desired protein concentration (p_1, p_2) .

Discussion

In this paper, we have characterized the extent by which the products of different genes expressed from the same plasmid become coupled due to the limited availability of RNAP and ribosomes. This is a standard configuration used in the design of synthetic circuits that allows easy incorporation of modules to perform increasingly complex tasks. The extent of this coupling is substantial ranging from 60% when circuits are on medium copy number plasmids to 29% when circuits are on very low copy number plasmids. These effects can therefore be significant in the design of synthetic circuits even when assembled on low copy number plasmids. We discovered that this coupling is described by isocost lines, identifying quantities in the cellular economy of gene expression that play the same role as price and budget in microeconomics (12). The isocost line stems from the limited availability of RNAP and ribosomes in the transcription and translation processes. While the existence of the isocost line is not dependent on separation of resource pools between plasmid and chromosome, the slope of the line may be affected by this separation (see SI Section B3). Our results (Fig 1A and Fig 1B) indicate that the local depletion of resources plays a role in the extent of the coupling among gene expression levels, however, investigating how spatial proximity affects the extent of this coupling is beyond the scope of this work. Further studies considering either genes expressed from different plasmids or from different locations on the same plasmid may provide additional information on how the extent of the coupling changes with spatial proximity.

Although it has been observed that gratuitous protein expression affects host growth (17, 18), it has also been shown that such effects are largely dependent on the protein expressed, the copy number, and the culture conditions such as the nutritional quality of the carbon source used (19–21). In particular, previous experiments performed in conditions similar to ours showed that these effects are only transient in the exponential phase and that they disappear after several generations of exponential growth (22). We performed all our experiments with very low (3-5), low (14-22), and medium (62-66) plasmid copy numbers, lower than the numbers commonly considered in previous works. Furthermore, we performed all our measurements at steady state after several generations of exponential growth. This combination of factors contributes to the rather modest change in growth rate that we have observed in our experiments upon AHL induction (Figs S22 and Fig S27).

The study of the isocost line also sheds light on the role that RNAP and ribosomes each play in the coupling of gene expression. When using an extremely weak RBS for the inducible gene (RFP), we do not observe a significant decrease in the expression of the other gene (GFP). This result indicates that the decrease in GFP is mostly due to the limited availability of ribosomes, in accordance with what was observed in studies *in vitro* (23). However, the increase in slope of the isocost line when the RBS strength for RFP is decreased (Fig 3A) cannot be predicted unless RNAP is limiting (for details, see SI Section B6). Our experimental results combined with our model indicate that the limited availability of RNAP manifests itself in a very subtle way. Specifically, a stronger RBS will allow a lower induction level to reach the same protein concentration. Lower induction, in turn, leads to lower demand for RNAP, which will then be available in higher concentrations to other genes, increasing their expression. This phenomenon, in which the limitation of RNAP plays a central role, controls the rotation of the isocost line.

Previous theoretical studies have analyzed how competition for common resources can affect the behavior of specific networks (24–26). In particular, Cookson *et al* (2011) modeled the sharing of common degradation machinery by multiple proteins and validated experimentally how this can alter the dynamic performance of synthetic circuits. Experimental demonstration of how this effect can be exploited to synchronize synthetic genetic oscillators was further demonstrated in (27). Mather *et al* (2013) proposed a stochastic model to capture the anticorrelation between protein counts due to mRNAs competing for ribosomes. Rondelez (2012) modeled enzymatic networks in which multiple substrates compete for the same enzyme and illustrated the dynamic effects of this competition on a synthetic oscillator called the metabolator. Except for the work of (24, 27), which studies competition for proteases as opposed to competition for RNAP and ribosomes, all the above works are purely theoretical and focus on modeling a specific system in which a species is competed for. By contrast, we

provide experimental results on a set of synthetic constructs especially designed to validate a general model prediction about both the extent of coupling among genes due to competition for RNAP and ribosomes and the key parameters that control this coupling. The analogy that we have established with economics is not exclusive to how transcriptional and translational resources are distributed in the process of gene expression. Metabolism itself has been viewed as a market with supply and demand blocks that share products (28). At a higher level, it has also been proposed that biological regulatory systems seek high performance while trying to be economical (29, 30).

Isocost lines will allow a deeper understanding of non-trivial interactions arising in natural systems, while being a step forward to the rational design of synthetic circuits. In particular, isocost lines establish a predictive framework for determining how circuit behavior is affected by competition for limited cellular resources and can be used as guidance for design.

Author Contributions

DDV, AG, JJ designed research; DDV, AG developed mathematical model; AG performed simulations; AG, JJ, HC performed experiments; JY, JJ, H-HH cloned constructs; DDV, RW, JJ, AG analyzed the data; DDV, AG, JJ wrote the paper.

Acknowledgments

We thank Adam J. Rubin for insights in conceiving this idea, Felix Moser for the gift of the DIAL strains and Shridhar Jayanthi for the helpful discussions. This work was supported by the AFOSR grant FA9550-12-1-0129, the DARPA contract W911NF-12-1-0540, and the NIH grant P50 GM098792. The authors declare that they have no conflict of interest.

Supporting Citations

References (31–45) appear in the supporting material.

References

- Hartwell, L. H., J. J. Hopfield, S. Leibler, and A. W. Murray, 1999. From molecular to modular cell biology. *Nature* 402:C47–52.
- Slusarczyk, A. L., A. Lin, and R. Weiss, 2012. Foundations for the design and implementation of synthetic genetic circuits. *Nature Rev. Genet.* 13:406–20.
- Cardinale, S., and A. P. Arkin, 2012. Contextualizing context for synthetic biology – identifying causes of failure of synthetic biological systems. *Biotechnol. J.* 7:856–66.
- Andrews, K. J., and G. D. Hegeman, 1976. Selective disadvantage of non-functional protein synthesis in *Escherichia coli*. *J. Mol. Evol.* 8:317–28.
- Bentley, W. E., N. Mirjalili, D. C. Andersen, R. H. Davis, and D. S. Kompala, 1990. Plasmid-encoded protein: The principal factor in the "metabolic burden" associated with recombinant bacteria. *Biotechnol. Bioeng.* 35:668–81.
- Klumpp, S., Z. Zhang, and T. Hwa, 2009. Growth rate-dependent global effects on gene expression in bacteria. *Cell* 139:1366–75.
- Koch, A. L., 1988. Why can't a cell grow infinitely fast? *Can. J. Microbiol.* 34:421–26.
- Scott, M., C. W. Gunderson, E. M. Mateescu, Z. Zhang, and T. Hwa, 2010. Interdependence of cell growth and gene expression: origins and consequences. *Science* 330:1099–1102.
- Jensen, K. F., and S. Pedersen, 1990. Metabolic growth rate control in *Escherichia coli* may be a consequence of subsaturation of the macromolecular biosynthetic apparatus with substrates and catalytic components. *Microbiol. Rev.* 54:89–100.
- Vind, J., M. A. Sorensen, M. D. Rasmussen, and S. Pedersen, 1993. Synthesis of proteins in *Escherichia coli* is limited by the concentration of free ribosomes: expression from reporter genes does not always reflect functional mRNA levels. *J. Mol. Biol.* 231:678–88.
- Churchward, G., H. Bremer, and R. Young, 1982. Transcription in bacteria at different DNA concentrations. *J. Bacteriol.* 150:572–81.
- Pyndick, R., and D. L. Rubinfeld, 2005. Microeconomics. Pearson Practice Hall, New Jersey, NJ.
- Kittleson, J. T., S. Cheung, and J. C. Anderson, 2011. Rapid optimization of gene dosage in *E. coli* using DIAL strains. *J. Biol. Eng.* 5.
- Akerlund, T., K. Nordstrom, and R. Bernander, 1995. Analysis of cell size and DNA content in exponentially growing and stationary-phase batch cultures of *Escherichia coli*. *J. Bacteriol.* 177:6791–97.
- Ishihama, Y., T. Schmidt, J. Rappsilber, M. Mann, F. U. Hartl, M. J. Kerner, and D. Frishman, 2008. Protein abundance profiling of the *Escherichia coli* cytosol. *BMC Genomics* 9.
- Nelson, K., T. Whittam, and R. K. Selander, 1991. Nucleotide polymorphism and evolution in the glyceraldehyde-3-phosphate dehydrogenase gene (*gapA*) in natural populations of *Salmonella* and *Escherichia coli*. *Proc. Natl. Acad. Sci. USA* 88:6667–71.
- Dong, H., L. Nilsson, and C. G. Kurland, 1995. Gratuitous overexpression of genes in *Escherichia coli* leads to growth inhibition and ribosome destruction. *J. Bacteriol.* 177:1497–1504.

18. Algar, R., T. Ellis, and G.-B. Stan, 2014. Modeling essential interactions between synthetic genes and their chassis cell. *In* IEEE Conference on Decision and Control.
19. Stoebel, D. M., A. M. Dean, and D. E. Dykhuizen, 2008. The cost of expression of *Escherichia coli lac* operon proteins is in the process, not in the products. *Genetics* 178:1653–60.
20. Carrera, J., G. Rodrigo, V. Singh, B. Kirov, and A. Jaramillo, 2011. Empirical model and in vivo characterization of the bacterial response to synthetic gene expression show that ribosome allocation limits growth rate. *Biotechnol. J.* 6:773–83.
21. Klumpp, S., and T. Hwa, 2014. Bacterial growth: global effects on gene expression, growth feedback and proteome partition. *Curr. Opin. Biotechnol.* 28:96–102.
22. Shachrai, I., A. Zaslaver, U. Alon, and E. Dekel, 2010. Cost of unneeded proteins in *E. coli* is reduced after several generations in exponential growth. *Mol. Cell.* 38:758–67.
23. Siegal-Gaskins, D., V. Noireaux, and R. M. Murray, 2013. Biomolecular resource utilization in elementary cell-free gene circuit. *In* American Control Conference. 1531–36.
24. Cookson, N. A., W. H. Mather, T. Danino, O. Mondragon-Palomino, R. J. Williams, L. S. Tsimring, and J. Hasty, 2011. Queueing up for enzymatic processing: correlated signaling through coupled degradation. *Mol. Syst. Biol.* 7:561.
25. Mather, W. H., J. Hasty, L. S. Tsimring, and R. J. Williams, 2013. Translational cross talk in gene networks. *Biophys. J.* 104:2564–72.
26. Rondelez, Y., 2012. Competition for catalytic resources alters biological network dynamics. *Phys. Rev. Lett.* 108:208102.
27. Prindle, A., J. Selimkhanov, H. Li, I. Razinkov, L. S. Tsimring, and J. Hasty, 2014. Rapid and tunable post-translational coupling of genetic circuits. *Nature* 508:387–91.
28. Hofmeyra, J.-H. S., and A. Cornish-Bowden, 2000. Regulating the cellular economy of supply and demand. *FEBS Lett.* 476:47–51.
29. Dekel, E., and U. Alon, 2005. Optimality and evolutionary tuning of the expression level of a protein. *Nature* 436:588–92.
30. Szekely, P., H. Sheftel, A. Mayo, and U. Alon, 2013. Evolutionary tradeoffs between economy and effectiveness in biological homeostasis systems. *PLoS Comput. Biol.* 9.
31. Gibson, D. G., L. Young, R.-Y. Chuang, J. C. Venter, C. A. Hutchison, and H. O. Smith, 2009. Enzymatic assembly of DNA molecules up to several hundred kilobases. *Nature Methods* 6:343–345. <http://dx.doi.org/10.1038/nmeth.1318>.
32. Chen, Y.-J., P. Liu, A. A. K. Nielsen, J. Brophy, K. Clancy, T. Peterson, and C. A. Voigt, 2013. Characterization of 582 natural and synthetic terminators and quantification of their design constraints. *Nature Methods* 10.
33. Datsenko, K. A., and B. L. Wanner, 2000. One-step inactivation of chromosomal genes in *Escherichia coli* K-12 using PCR products. *PNAS* 97.
34. Salis, H. M., E. A. Mirsky, and C. A. Voigt, 2009. Automated design of synthetic ribosome binding sites to control protein expression. *Nature Biotechnol.* 27:946–950. <http://dx.doi.org/10.1038/nbt.1568>.
35. Salis, H. M., 2011. Chapter two - The Ribosome Binding Site Calculator. *In* C. Voigt, editor, *Synthetic Biology, Part B Computer Aided Design and DNA Assembly*, Academic Press, volume 498 of *Methods in Enzymol.*, 19 – 42. <http://www.sciencedirect.com/science/article/pii/B9780123851208000024>.
36. Arkin, A. P., J. Ross, and H. H. McAdams, 1998. Stochastic kinetic analysis of developmental pathway bifurcation in phage λ -infected *Escherichia coli* cells. *Genetics* 194.
37. Klumpp, S., and T. Hwa, 2008. Growth-rate-dependent partitioning of RNA polymerases in bacteria. *Proc. Natl. Acad. Sci. USA* 105:20245–50.
38. Bremer, H., and P. P. Dennis, 1996. Modulation of chemical composition and other parameters of the cell growth rate, in *Escherichia coli and Salmonella*, American Society for Microbiology, Washington, DC, chapter 97, 1553–69.
39. Tsien, R. Y., 1998. The green fluorescent protein. *Annu. Rev. Biochem.* 67.
40. Bernstein, J. A., A. B. Khodursky, P.-H. Lin, S. Lin-Chao, and S. N. Cohen, 2002. Global analysis of mRNA decay and abundance in *Escherichia coli* at single-gene resolution using two-color fluorescent DNA microarrays. *Proc. Acad. Natl. Sci. USA* 99.
41. Kramer, G., R. R. Sprenger, M. A. Nessen, W. Roseboom, D. Speijer, L. de Jong, M. J. T. de Mattos, J. W. Back, and C. G. de Koster, 2010. Proteome-wide alterations in *Escherichia coli* translation rates upon anaerobiosis. *Mol. Cell. Proteomics* 9.
42. Bremer, H., P. P. Dennis, and M. Ehrenberg, 2003. Free RNA polymerase and modeling global transcription in *Escherichia coli*. *Biochimie* 85.
43. Tunitskaya, V., and S. Kochetkov, 2002. Structural-functional analysis of bacteriophage T7 RNA polymerase. *Biochem. (Mosc.)* 67.
44. Deuschle, U., W. Kammerer, R. Gentz, and H. Bujard, 1986. Promoters of *Escherichia coli*: a hierarchy of in vivo strength indicates alternate structures. *EMBO J.* 5.
45. den Boom, T. V., and J. E. C. Jr., 1989. Genetics and regulation of bacterial lipid metabolism. *Annu. Rev. Microbiol.* 43.

Supporting Material

An online supplement to this article can be found by visiting BJ Online at <http://www.biophysj.org>.